Fragmentation patterns of 4(5)-nitroimidazole and 1-methyl-5-nitroimidazole – the effect of the methylation

Eero Itälä[a], Katrin Tanzer[b], Sari Granroth[a], Kuno Kooser[a], Stephan Paul Denifl[b], Edwin Kukk[a]

[a] *Department of Physics and Astronomy, University of Turku, FI-20014, Turku, (Finland)*

[b] *Institut für Ionenphysik und Angewandte Physik and Center of Molecular Biosciences, Leopold Franzens Universität Innsbruck, Technikerstrasse 25, 6020 Innsbruck (Austria)*

Corresponding author: Eero Itälä (ersita@utu.fi)

Abstract

We present here the photofragmentation patterns of doubly ionized 4(5)-nitroimidazole and 1-methyl-5-nitroimidazole. The doubly ionized state was created by core ionizing the C 1s orbitals of the samples, rapidly followed by Auger decay. Due to the recent development of nitroimidazole-based radiosensitizing drugs, core ionization was selected as it represents the very same processes taking place under the irradiation with medical X-rays. In addition to the fragmentation patterns of the sample, we study the effects of methylation on the fragmentation patterns of nitroimidazoles. We found that methylation alters the fragmentation significantly, especially the charge distribution between the final fragments. The most characteristic feature of the methylation is that it effectively quenches the production of NO and NO^+, widely regarded as key radicals in the chemistry of radiosensitization by the nitroimidazoles.

1 Introduction

Nitroimidazoles are commonly used as antibacterial drugs such as antibiotics and recently these compounds have also been tested as radiosensitizers in radiation therapy [1, 2]. In particular, some nitroimidazoles have proven to be effective when treating hypoxic tumors, where the target area is

deprived of oxygen and therefore resistant to the effects of radiation therapy. Clinical trials have concentrated on misonidazole (a 2-nitroimidazole), metronidazole (a 2-methyl-5-nitroimidazole) and nimorazole (a 5-nitroimidazole). Although misonidazole was proven to be an effective radiosensitizer (in contrast to metronidazole), it was also found to be neurotoxic and hence useless in combination with radiation therapy [3, 4, 5, 6, 7]. Nimorazole, on the other hand, provided very promising results [8] and is at the moment being used in Denmark and Norway in routine clinical practice and studied on human subjects by the Cancer Research UK. Regardless of the potential of nitroimidazoles as radiosensitizers, very little is known on how ionizing radiation affects nitroimidazoles.

Until recently, only few gas-phase studies with nitroimidazoles could be found, such as the ones by Kajfež *et. al.* and Jimenez *et. al.* who studied photoelectron spectroscopy (PES) and mass analyzed kinetic energy spectra (MIKE) studies of 4(5)-nitroimidazole [9, 10]. However, a few years ago Yu *et. al.* reported on the decomposition of nitroimidazolic compounds [11] and in 2014 Feketeová *et. al.* published a mass spectrometry study on the formation of radical anions in nitroimidazolic compounds [12]. Shortly after this, Tanzer *et. al.* showed that methylation of nitroimidazole at the N1 site completely blocks the rich chemistry induced by the attachment of low energy free electrons [13]. In 2015, a study on 2- and 4(5)-nitroimidazole ions using collision induced dissociation (CID) and electron induced dissociation (EID) reported different fragmentation in 2- and 4(5)-nitroimidazole in the case of EID [14].

All the above studies represent mostly the indirect effects of ionizing radiation and concern single ionization. This is regardless of the fact that medical X-rays induce primarily core ionization which is followed by Auger electron ejection leading to a doubly ionized molecule. Thus we report here the first results on the fragmentation of doubly ionized nitroimidazoles, namely 4(5)-nitroimidazole (4(5)NIZ) and 1-methyl-5-nitroimidazole (1Me5NIZ). As among the clinically studied samples, the methylated nitroimidazole is the weakest radiosensitizer, we chose to study here how the methylation affects the fragmentation of 4(5)-nitroimidazole. Combined with the previous results, this information helps us to understand how nitroimidazoles act as radiosensitizers in radiation therapy.

The skeletal formulae of the sample molecules are presented in Figure 1; 5NIZ isomer does not exist in the condensed phase, but tautomerizes spontaneously to its 4NIZ isomer [14]. Upon evaporation, however, 4NIZ partially undergoes isomerization into 5-nitroimidazole resulting in the molecular ratio of 1:0.70 of 4NIZ to 5NIZ [15]. To our knowledge, the 1Me5NIZ does not undergo any isomerization when evaporated.

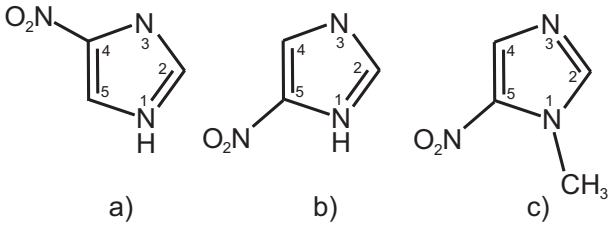

Figure 1: The skeletal formulae of the studied samples, 4NIZ (a), 5NIZ (b) and 1Me5NIZ (c).

2 Experimental

The experimental method employed here is electron-energy-resolved (photo)electron-(photo)ion-(photo)ion coincidence (PEPIPICO) spectroscopy [16, 17, 18]. In the PEPIPICO experiments, we used a custom-made Wiley-McLaren type ion time-of-flight (TOF) spectrometer and a hemispherical electron energy analyzer Omicron EA-125 with 125 mm nominal radius. The electron analyzer was re-equipped with a fast position sensitive resistive anode readout based on 40 mm active diameter microchannel plate detector (Quantar Inc.). Also new electronics and software for recording the electron detector signal and controlling electron lens and hemisphere electrodes was developed, resulting in enhanced transmission of the analyzer and better optimization options. More details on the coincidence setup can be found in Ref. [19]. The experiment was performed at the soft X-ray beamline I411 at the MAX-II synchrotron [20], using monochromatized radiation of 317 eV photon energy. The molecules were sublimated and transferred into the sample area using an effusion cell with integrated cooling shroud (MBE Komponenten NTEZ40 oven) keeping the temperature below 110 °C for 4-NIZ and 41 °C for 1Me5NIZ. The 4-NIZ and 1Me5NIZ samples were purchased from Sigma Aldrich and were used "as is" with the stated purities being $\geq 99\%$.

The electron analyzer was operated at 100 eV pass energy using 6 mm entrance slit, which provided instrumental resolution of about 2.40 eV (FWHM). During the coincidence measurement with the C 1s photoelectrons, the analyzer was tuned to capture the kinetic energy window from 17 to 29 eV. The ion TOF spectrometer was operated under Wiley-McLaren conditions, applying -707 V potentials to the drift tube and ± 100 V to the ion extraction grids. The start triggers for the ion TOF measurement in pulsed extraction field mode were provided by the electron detector. In order to reduce the contribution from so-called "false" coincidences [20], low ionization rates were used with about 20 electrons/s counted. In addition, artificial triggers were generated to record PIPICO events that contain only the false coincidences; these were then used for subtracting false coincidence background from the PEPIPICO maps.

3 Discussion

The absorption of a 317 eV photon by 4(5)NIZ or 1Me5NIZ induces C 1s core ionization which is followed by Auger electron ejection in $\tau \sim 10fs$ [21]. This leaves the molecule in a highly unstable doubly charged state which relaxes via fragmentation into two momentum-correlated cations and a number (or none) of neutral species. To determine the exact fragmentation pathways of these processes, we have used the so-called PEPIPICO maps to analyze the experimental data. More detailed description of such maps and how to interpret them can be found *e.g.* in Ref. [22]. Briefly, the TOFs of the ions in a charged fragment pair are plotted versus each other, the faster ion on the X-axis and the slower ion on the Y-axis. Due to the approximately isotropic initial velocity vector and the momentum correlation, the ion pairs appear on the PEPIPICO map as tilted cigar-shaped "islands". The center coordinates of each pattern corresponds to the nominal flight times of the coincident fragments with no velocity and the slopes of the sequence depend on the fragmentation pathway. Each pattern thus describes different fragmentation process, the intensity of which can be determined by counting all the events in it. The error bars for the intensities were taken as statistic uncertainties of these numbers of events.

We focus here on how methylation of 5NIZ alters its fragmentation. This is done by comparing the fragmentation patterns of 4(5)NIZ and 1Me5NIZ with the assumption that the fragmentation of the two isomers (4NIZ and 5NIZ) is essentially similar following C 1s core ionization. This is different from the case of valence ionization where the branching ratios of different fragmentation channels differ between 4NIZ and 5NIZ. This difference is due to the energies of the molecular orbitals, which are not identical for 4NIZ and 5NIZ [15]. In other words, in valence ionization, the fragmentation is very sensitive to the amount of internal energy (IE) the molecule is left with after the ionization. In core ionization the situation is totally different since there the amount of internal energy involved in the process is significantly larger and slight IE deviations become insignificant. For this reason, the results presented here are expected to concern the effects of the methylation in general, regardless of the initial site of the methyl group.

3.1 Fragmentation of 4(5)-nitroimidazole

The PEPIPICO map of 4(5)NIZ is depicted in Fig. 2 and the ion pairs corresponding to the patterns are presented in Table 1 together with their relative intensities. Those pairs with intensities less than 0.5 % of the total intensity of the PEPIPICO map are excluded from Table 1. Therefore the total intensity of the ion pairs presented in Table 1 is below 100%. Although the PEPIPICO map is rich with patterns, the biggest contribution of the maps total intensity is due to only a few fragmentation

channels, all involving the NO^+ production. Before discussing any further the significance of NO^+, let us go through the whole fragmentation scheme, which is quite straightforward.

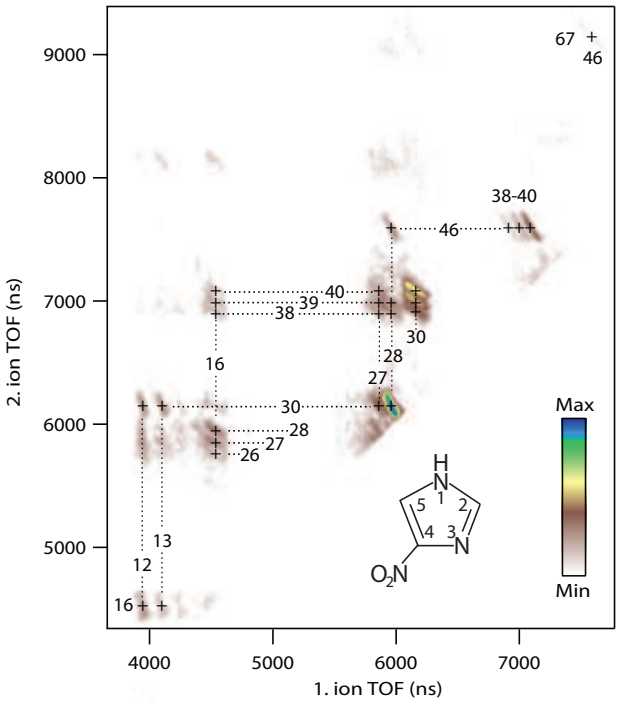

Figure 2: PEPIPICO map of 4(5)-nitroimidazole, the color scale of the map has been adjusted so that the intensities of the weak patterns are enhanced.

Table 1: Coincident ion pairs following the fragmentation of 4(5)-NIZ dication. Those pairs with intensity of 0.5% or less are not shown.

Masses (amu)	Fragment1	Fragment2	Intensity (%)	Masses (amu)	Fragment1	Fragment2	Intensity (%)
(12, 16)	C^+	O^+	2.11±0.2	(27, 30)	CHN^+	NO^+	3.83±0.2
(13, 16)	CH^+	O^+	1.12±0.1	(28, 30)	CH_2N^+	NO^+	26.08±0.4
(14, 16)	CH_2^+/N^+	O^+	0.78±0.1	(27, 38)	CHN^+	C_2N^+	2.19±0.2
(12, 27)	C^+	CHN^+	1.63±0.1	(27, 39)	CHN^+	C_2HN^+	2.29±0.2
(12, 28)	C^+	CH_2N^+	1.30±0.1	(27, 40)	CHN^+	$C_2H_2N^+$	1.29±0.1
(12, 30)	C^+	NO^+	2.03±0.2	(28, 38)	CH_2N^+	C_2N^+	2.56±0.2
(13, 30)	CH^+	NO^+	1.99±0.2	(28, 39)	CH_2N^+	C_2HN^+	3.08±0.2
(16, 26)	O^+	CN^+	2.63±0.2	(30, 38)	NO^+	C_2N^+	5.94±0.2
(16, 27)	O^+	CHN^+	2.97±0.2	(30, 39)	NO^+	C_2HN^+	7.75±0.3
(16, 28)	O^+	CH_2N^+	1.42±0.1	(30, 40)	NO^+	$C_2H_2N^+$	10.46±0.3
(16, 38)	O^+	C_2N^+	1.55±0.1	(28, 46)	CH_2N^+	NO_2^+	2.19±0.2
(16, 39)	O^+	C_2HN^+	0.95±0.1	(38, 46)	C_2N^+	NO_2^+	0.88±0.1
(16, 40)	O^+	$C_2H_2N^+$	2.11±0.2	(39, 46)	C_2HN^+	NO_2^+	1.51±0.1
(27, 28)	CHN^+	CH_2N^+	3.19±0.2	(40, 46)	$C_2H_2N^+$	NO_2^+	4.14±0.2

Figure 3 presents all the fragmentation channels producing the patterns on the PEPIPICO map of Fig. 2. As seen, the fragmentation of 4(5)NIZ always begins by the ejection of neutral or cationic nitro (NO_2) group. In the case of cationic NO_2 ejection, it is very likely that the NO_2^+ fragments upon the ejection. Regardless of the charge distribution after the first step and whether or not the NO_2^+ fragments during the ejection, the second step of the fragmentation always is similar; the imidazole ring fragments via the rupture of C5-N1 and C2-N3 bonds.

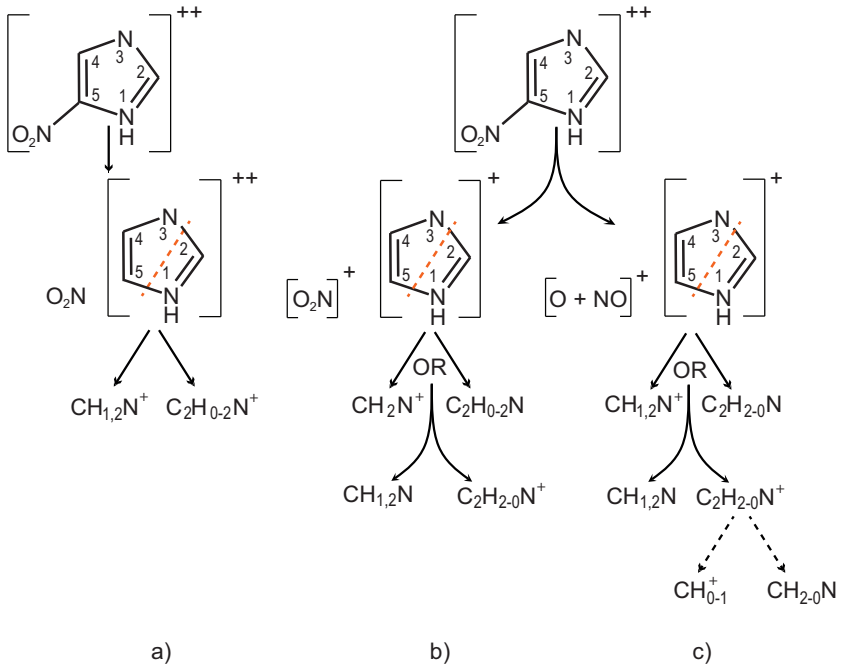

Figure 3: Fragmentation pathways of 5NIZ leading to the detected coincident ion pairs. As the pathways for 4NIZ and 5NIZ follow the same bond cleavages after the ejection of the nitro group, only the pathways for 5NIZ have been illustrated here.

If the nitro group is ejected as neutral specie, the charge separation takes place in the second step producing CH_nN^+ (n=1,2) in coincidence with $C_2H_nN^+$ (n=0-2), pairs (27-28, 38-40) as presented in Fig. 3 (a). NO_2^+ ejection involves charge separation in the first step; if the nitro group stays intact, (28, 46) and (38-40, 46) fragments are produced. Now only one of the fragments CH_nN (n=1,2) or C_2H_nN (n=0-2) obtains positive charge (see Fig. 3 (b)), if the positive charge goes to CH_nN, the only possible assignment is where n=2, CH_2N^+.

As one can easily obtain from the PEPIPICO map and from the Table 1, the most common fragmentation pathway for the doubly charged 4(5)NIZ is that of Fig. 3 (c). This pathway has a probability of over 70%. The remaining PEPIPICO patterns are produced via this process. There the NO_2^+ fragments during the ejection either into NO^+ and O (clearly the most common option) or into O^+ and NO. Either way, the fragmentation after the charge separation follows the same

scheme depicted in the Figure 3 (c). What is also noteworthy here is the possible (although unlikely) further fragmentation of the $C_2H_nN^+$.

3.2 Fragmentation of 1-methyl-5-nitroimidazole

The PEPIPICO map of 1Me5NIZ is depicted in Fig. 4 and the ion pairs corresponding to the patterns are presented in Table 2 together with the relative intensities of the ion pairs. Similarly to 4(5)-NIZ, those pairs with intensities less than 0.5 % of the total intensity of the PEPIPICO map are excluded from the Table. The PEPIPICO map is strongly characterized by the 15 and 29 amu fragments, possibly CH_3^+ and $C_2H_3^+$ respectively. However, closer analysis reveals that such simplification cannot be made and the fragmentation of 1Me5NIZ does not follow any general model. Instead, the PEPIPICO patterns correspond to a very large variety of different fragmentation pathways and bond cleavages. Only one thing is common for most of these pathways: the ejection of the nitro group at the first step of the fragmentation.

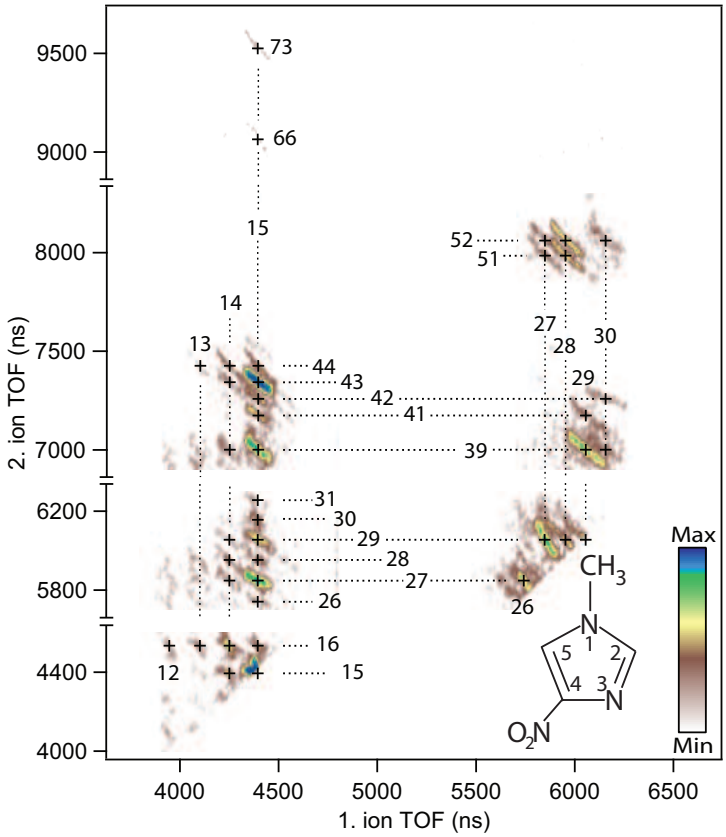

Figure 4: PEPIPICO map of 1-methyl-5-nitroimidazole, the color scale of the map has been adjusted so that the intensities of the weak patterns are enhanced.

Due to the large variety of the fragmentation channels, we do not discuss all the channels in

Table 2: Coincident ion pairs following the fragmentation of 1Me5NIZ dication. Those pairs with intensity of 0.5% or less are not shown.

Masses (amu)	Fragment1	Fragment2	Intensity (%)	Masses (amu)	Fragment1	Fragment2	Intensity (%)
(12,16)	C^+	O^+	0.68±0.1	(15,39)	NH^+	C_2HN^+	6.78±0.3
(13,16)	CH^+	O^+	0.91±0.1	(15,41)	CH_3^+	CHN_2^+	2.30±0.1
(14,16)	CH_2^+/N^+	O^+	2.11±0.1	(15,42)	NH^+	CNO^+	1.61±0.1
(15,16)	CH_3^+/NH^+	O^+	1.50±0.1	(15,43)	NH^+	$CHNO^+$	8.57±0.3
(14,15)	N^+	NH^+	1.46±0.1	(15,44)	NH^+	CH_2NO^+	1.26±0.1
(15,15)	NH^+	NH^+	6.55±0.2	(26,27)	CN^+	CHN^+	2.34±0.1
(14,27)	N^+	CHN^+	1.47±0.1	(27,29)	CHN^+	CH_3N^+	6.43±0.2
(14,28)	N^+	CH_2N^+	1.52±0.1	(28,29)	CH_2N^+	CH_3N^+	2.40±0.1
(14,29)	N^+	CH_3N^+	1.04±0.1	(29,29)	CH_3N^+	CH_3N^+	1.69±0.1
(15,26)	NH^+	CN^+	1.38±0.1	(29,39)	CH_3N^+	C_2HN^+	7.15±0.3
(15,27)	NH^+	CHN^+	7.05±0.2	(29,41)	CH_3N^+	$C_2H_3N^+$	2.33±0.1
(15,28)	NH^+	CH_2N^+	2.73±0.1	(30,39)	NO^+	C_2HN^+	2.62±0.1
(15,29)	NH^+	CH_3N^+	3.92±0.2	(30,42)	NO^+	CNO^+	1.79±0.1
(15,30)	NH^+	NO^+	1.73±0.1	(27,51)	CHN^+	C_3HN^+	1.89±0.1
(14,39)	CH_2^+/N^+	C_2HN^+	1.80±0.1	(27,52)	CHN^+	$C_3H_2N^+$	2.62±0.1
(14,43)	CH_2^+/N^+	$CHNO^+$	1.03±0.1	(25,51)	CH_2N^+	C_3HN^+	2.96±0.1
(14,44)	CH_2^+/N^+	CH_2NO^+	1.21±0.1	(28,52)	CH_2N^+	$C_3H_2N^+$	3.33±0.1
				(30,52)	NO^+	$C_3H_2N^+$	1.77±0.1

detail. Instead, we concentrate on the dominating ones, which are presented in Figure 5. The (27-28, 51-52) pairs correspond to the very simple process (a), which is basically identical to that of Fig. 3 (a). Process (b) of Fig. 5 corresponds to the (27, 29), (29, 39) and (29, 41) fragments; also this process is quite straightforward, the NO_2 ejection is again followed by charge separation into $C_3H_3N^+$ and CH_3N^+, after which the $C_3H_3N^+$ fragments further into $C_2H_{1,3}N^+$ and CHN^+.

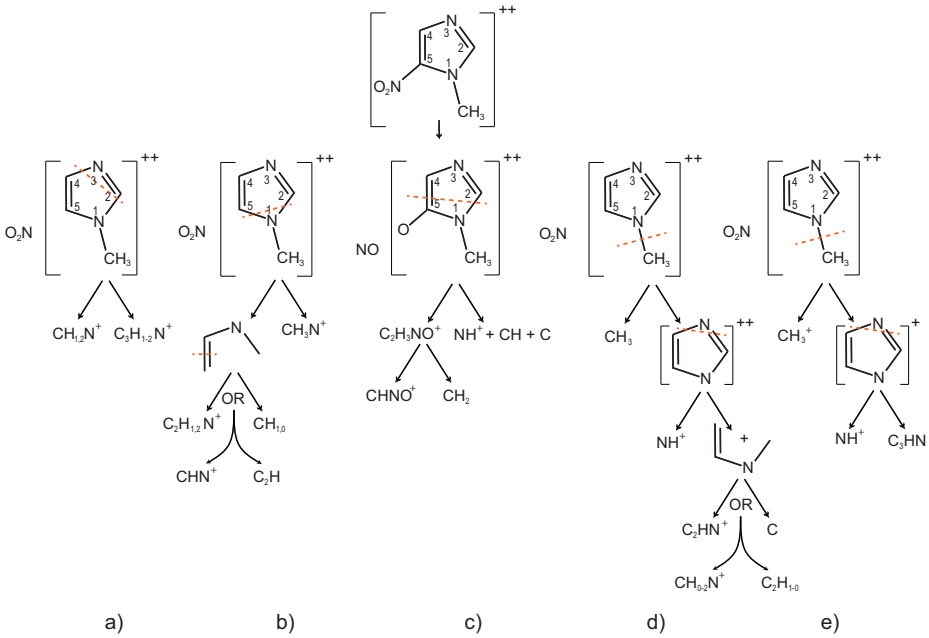

Figure 5: Five of the most common fragmentation channels of doubly charged 1Me5NIZ.

There are several common fragmentation channels producing a 15 amu fragment, which, perhaps a little surprisingly, is usually NH^+. For example the channel (c) of Fig. 5 results in NH^+ in

coincidence with $CHNO^+$. This process involves the attachment of one of the oxygens of the nitro group to the C2 upon the ejection of the nitro group. Interestingly, when we compare 1Me5NIZ and 5NIZ, we notice that this process distinctively describes the fragmentation of singly ionized nitroimidazole, but is totally absent when double ionization is considered. The process (d) of Figure 5 produces either CH_nN^+ (n=0-2) or C_2HN^+ in coincidence with NH^+; The first step is again the NO_2 release which is then followed by the ejection of the methyl group. The charge separation takes place on the third step after which the final fragments are produced in the fourth step. One should note that the formation of (NH^+, CH_2N^+) pair (which is a very rare process) requires hydrogen migration from the methyl group. The characteristic pattern corresponding to (15, 15) follows the pathway (e) which is very similar to (d). The difference is, that now the charge separation takes place in the second step (CH_3^+ ejection). This is then followed by the further fragmentation of the imidazole ring and the production of NH^+. The shape of the pattern is due to the superimposition of two ion patterns with different slopes. Such effect is possible when the coincident fragments masses are equal [22].

3.3 The effect of the methylation

Let us now consider, how the methylation influences on the fragmentation of 5-nitroimidazole. Regardless of the methylation, the first step of the fragmentation of doubly charged nitroimidazole is essentially the same, the ejection of the nitro group. However, apart from the one shared fragmentation channel (Fig. 3 (a) of NIZ and 5 (a) of 1Me5NIZ), the fragmentation scheme after the first step changes due to methylation. Although NIZ and 1Me5NIZ eventually produce also the same fragments such as CH_nN^+ and $C_2H_nN^+$, these fragments actually result from very different pathways. As Figures 3 and 5 show, methylation allows new bond cleavages during the fragmentation, but it also influences on the ejection of the nitro group. In the case of nitroimidazole, NO_2 is usually ejected as a cation, which breaks up upon the ejection, resulting in NO^+ production. In 1Me5NIZ, however, the NO_2 is characteristically ejected as neutral intact moiety.

Methylation of nitroimidazole thus essentially prevents the positive charge localization to the nitro group upon its ejection. Figure 6 further illustrates how effectively methylation suppresses the charge localization to the nitro group and the production of NO/NO^+. The red bars represent all the fragmentation channels, whereas the yellow ones describe those channels where the nitro group is ejected as a cation. The brown bars describe the neutral or charged NO production.

The dramatic drop in the NO/NO^+ yield is clearly the most distinctive feature of the methylation; could this be connected to the radiosensitizing properties of nitroimidazoles? It was mentioned

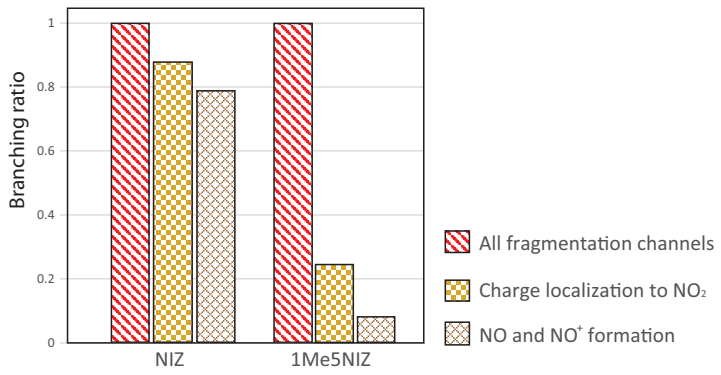

Figure 6: The branching ratios (with respect to the total ion yield (red bar)) for the fragmentation pathways where the charge localizes to the nitro group (yellow bar) and for the processes producing NO or NO^+ (brown bar). As seen, the charge localization to the nitro group and the NO/NO^+ production is strongly suppressed as a result of methylation.

earlier, that methylated nitroimidazole, metronidazole, has not been proven to be very good radiosenstizer [1], unlike those nitroimidazoles that do not contain the methyl group. The NO/NO^+ production efficiency upon ionization thus seems to be connected to the radiosenstizing abilities of nitroimidazoles. The main theory concerning radiation damage is that the irreversible damage induced by ionizing radiation is mainly due to DNA damage that is made permanent by the present oxygen via peroxy radical formation, which eventually leads to cell inactivation or mutation [23, 24]. In hypoxic tumors the oxygen level is very low: This decreases the false DNA repair and increases the tumor cells' resistance against the destructive effects of ionizing radiation. As NO is a very efficient oxidizer and is considered to be even more effective radiosensitizer than oxygen [25], a tentative conclusion could be drawn from the present results and the clinical ones concerning the function of nitroimidazole as radiosensitizers. Their effectiveness could be based on the (neutral and cationic) production of NO, which mimic the function of oxygen: when the hypoxic cells are irradiated with ionizing radiation, NO fixes the damaged DNA leading to increased cell inactivation. The effect of NO on non-hypoxic cells is not so significant, because there the oxygen already acts as a radiosensitizer.

4 Conclusions

The fragmentation of 4(5)-nitroimidazole and its methylated derivative, 1-methyl-5-nitroimidazole, induced by C 1s core ionization was studied. The fragmentation of both molecules is characterized

by the ejection of the nitro group at the first step of the fragmentation. However, after the first step, the fragmentation schemes are very different. In the case of 4(5)-NIZ the nitro group is ejected as a cation, and fragments during the ejection, whereas in the case of 1Me5NIZ the nitro group is ejected as a neutral molecule. This is also the reason for the most notable effect of the methylation; it suppresses the NO and NO^+ production very efficiently.

Radiation damage involves various, often complex processes that cannot be strictly compared to the situation of isolated molecules. Also, direct interaction such as core ionization is responsible for less than 50 % of the total damage induced by ionizing radiation, the main contribution comes from indirect processes such as inelastic electron scattering [26, 27]. However, the results presented here can still help understanding the chemistry that takes place when nitroimidazolic drugs are used in combination with radiation therapy. Clinical studies have concluded that a methylated nitroimidazole, metronidazole, is not very effective radiosensitizer. This leads us to believe that the NO/NO^+ production upon core ionization is a significant feature for effective nitroimidazolic radiosensitizers, even in solution such as water (*cf.* human tissue). As NO is an effective oxidizer, the delivery of nitroimidazole into the hypoxic tumors thus helps re-oxygenating the tumor cells upon irradiation with ionizing radiation. This, in turn, increases the DNA damage to the tumor cells together with the reactive radicals also generated as result of the fragmentation of doubly charged nitroimidazoles.

References

[1] Oronsky, B. T.; Knox, S. J.; Scicinski, J. J.; *Transl. Oncol.* **2011**, *4*, 189198.

[2] Overgaard, J.; *Radiother. Oncol.* **2011**, *1*00, 22.

[3] Brown, J. M.; *Radiat. Res.* **1975**, *6*4, 633647.

[4] Dische, S.; Saunders, M. I.; Lee, M. E.; Adams, G. E.; Flockhart, I. R.; *Br. J. Cancer.* **1977**, *3*5, 567579.

[5] Brown, J. M. ; *Int. J. Radiat. Oncol. Biol. Phys.* **1984**, *1*0, 425429.

[6] Rosenberg, A.; Knox, S.; *Int. J. Radiat. Oncol. Biol. Phys.* **2006**, *6*4 343354.

[7] Overgaard, J.; Sand Hansen, H.; Andersen, A. P.; Hjelm-Hansen, M.; Jørgensen, K.; Sandberg, E.; Berthelsen, A.; Hammer, R.; Pedersen, M.; *Int, J, Radiat, Oncol, Biol, Phys.* **1989**, *1*6, 1065-1068

[8] Overgaard, J.; Sand Hansen, H.; Overgaard, M.; Bastholt, L.; Berthelsen, A.; Specht, L.; Lindeløv, B.; Jørgensen, K.; *Radiother. Oncol.* **1998**, *4*6, 135-146.

[9] Kajfež, F.; Klasinc, L.; Šunjić, V.; *J. Heterocycl. Chem.* **1979**, *1*6, 529.

[10] Jimenez, P.; Laynes, J.; Claramunt, R. M.; Sanz, D.; Fayet, J. P.; Vertut, M. C.; Catalán, J.; de Paz, J. L. G.; Pfister-Guillouzo, G.; Guimon, C.; Flammang, R.; Maquestiau, A.; Elguero, J.; *New J. Chem.* **1989**, *1*3, 151.

[11] Yu, Z.; Bernstein, E. R.; *J. Chem. Phys.* **2012**, *1*37, 114303.

[12] Feketeová, L.; Albright, A. L.; Sørensen, B. S.; Horsman, M. R.; White, J.; OHair, R. A. J.; Bassler, N.; *Int. J. Mass Spectrom.* **2014**, *365366*, 56.

[13] Tanzer, K.; Feketeová, L.; Puschnigg, B.; Scheier, P.; Illenberger, E.; Denifl, S.; *Angew. Chem., Int. Ed.* **2014**, *5*3, 12240.

[14] Feketeová, L.; Postler, J.; Zavras, A.; Scheier, P.; Denifl, S.; OHair, R. A. J.; *Phys. Chem. Chem. Phys.* **2015**, *1*7, 12598.

[15] Feketeová, L.; Plekan, O.; Goonewardane, M.; Ahmed, M.; Albright, A. L.; White, J.; OHair, R. A. J.; Horsman, M. R.; Wang, F.; Prince, K. C.; *J. Phys. Chem. A* **2015**, *1*19, 9986-9995.

[16] Frontiers of Coincidence Experiments, (edited by K. Ueda) Elsevier, Amsterdam, 2004.

[17] Danby, C. J.; Eland, J. H. D.; *Int. J. Mass Spectrom. and Ion Phys.* **1972**, *8*, 153-161.

[18] Hitchcock, A. and Neville, J. in *Chemical Applications of Synchrotron Radiation: I*, ed. by T. Sham (World Scientific, Singapore, 2002).

[19] Kukk, E.; Sankari, R.; Huttula, M. ; Sankari, A.; Aksela, H.; Aksela, S; *J. Electron Spectrosc. Relat. Phenom.* **2007**, *1*55, 141.

[20] Prümper, G.; Ueda, K.; *Nucl. Instrum. Methods. Phys. res. Sect. A* **2007**, *5*74, 350.

[21] Coville, M.; Thomas, D. T.; *Phys. Rev. A.* **1991**, *4*3, 6053-6056.

[22] Itälä, E.; Kukk, E.; Ha, D. T.; Granroth, S.; Caló, A.; Partanen, L.; Aksela, H.; Aksela S.; *J. Chem. Phys.* **2009**, *1*31, 114314.

[23] Howard-Flanders, P.; Alper, T.; *Radiat. Res.* **1957**, *7*, 518540.

[24] Radiobiology For The Radiologist 6th ed. (E. Hall and A. Giaccia) Lippincott William and Wilkins: Philadelphia, 2006.

[25] Oronsky, B. T.; Knox, S. J.; Scicinski, J. J.; *Transl. Oncol.* **2012**, *5*, 66-71.

[26] Baccarelli, I.; Bald, I.; Gianturco, F. A.; Illenberger, E.; Kopyra, J.; *Phys. Rep.* **2011**, *5*08, 144.

[27] Sanche, L.; *Europ. J. Phys. D* **2005**, *3*5, 367390.